Title

Cartilage and chondrocyte response to extreme muscular loading and impact loading: Can *in vivo* pre-load decrease impact-induced cell death?

Running titles

Muscular pre-loading affects impact-induced cell death

Authors

Douglas A. Bourne[1], Eng Kuan Moo[1], Walter Herzog[1]

Affiliations:

1. Human Performance Laboratory, Faculty of Kinesiology, The University of Calgary, Calgary, Alberta, Canada

Corresponding author

Walter Herzog

Human Performance Laboratory, The University of Calgary

2500 University Drive NW, Calgary, Alberta, T2N 1N4, Canada

Tel: +1 403 220 8525; Email: wherzog@ucalgary.ca

Word count: 279 words (abstract), 4671 words (main text)

Abstract:

Background: Impact loading is a risk factor for cartilage damage and cell death. Pre-loading prior to impact loading may protect cartilage and chondrocytes. However, there is no systematic evidence on the effects of pre-load strategies on cartilage damage and chondrocyte death, nor is there an understanding of why and how pre-loads might protect cartilage and chondrocytes from impact-induced damage. This study aimed at determining the effects of the pre-load history on impact-induced chondrocyte death in an intact joint.

Methods: Patellofemoral joints from 42 rabbits were loaded by controlled quadriceps muscle contractions and an external impacter. Two extreme muscular loading conditions were used: (i) a short-duration, high intensity, static muscle contraction, and (ii) a long-duration, low-intensity, cyclic muscle loading protocol. A 5-Joule centrally-oriented, gravity-accelerated impact load was applied to the patellofemoral joint. Local chondrocyte viability was quantified following the muscular loading protocols, following application of the isolated impact loads, and following application of the impact loads that were preceded by the muscular pre-loading conditions. Joint contact pressures were also measured for all loading conditions by a pressure-sensitive film.

Findings: Comparing to cartilage injured by impact loading alone, cartilage pre-loaded by static, maximal intensity, short-term muscle loads had lower cell death, while cartilage pre-loaded by repetitive, sub-maximal intensity, long-term muscular loads has higher cell death. The locations of peak joint contact pressures were not strongly correlated with the locations of greatest cell death occurrence.

Interpretation: Static, high intensity, but short muscular pre-load protected cells from impact injury; whereas repetitive, low intensity, but prolonged muscular pre-loading to the point of

muscular fatigue left the chondrocytes vulnerable to injury. However, cell death does not seem to be related to the peak joint pressures.

Keywords: chondrocyte death, joint contact pressure, osteoarthritis, patellofemoral joint, pre-loading

Introduction

Injuries to cartilage are thought to trigger the development of a debilitating joint disease called post-traumatic osteoarthritis (PTOA) (Anderson et al., 2011; Dirschl et al., 2004). PTOA not only affects the quality of life of patients, it also imposes a substantial financial burden on the health care system, primarily because of the long-term conservative rehabilitation requirements and the large number of joint replacement surgeries performed today (Wieland et al., 2005).

Injuries to articular cartilage are often characterized by fissures in the extracellular matrix (ECM) (Chen et al., 2001a; Dirschl et al., 2004; Ewers et al., 2001; Krueger et al., 2003; Lewis et al., 2003; Rundell et al., 2005; Szczodry et al., 2009). Such fissures result in mechanical weakening and associated loss of protective properties for the chondrocytes. If ECM damage is substantial, it typically results in cell death and associated degeneration of the adjacent cartilage tissue (Shlopov et al., 1997). Most cases of OA are associated with extensive cell death resulting in a decrease in the overall number of cells, and a concomitant failure of the remaining cells to maintain normal tissue homeostasis (Aigner et al., 2007; Blanco et al., 1998; Hashimoto et al., 1998). Thus, it is believed that preventing chondrocyte loss is a key factor in the maintenance of cartilage health and the prevention of the onset and rapid progression of OA.

Impact loading has been identified as a primary risk factor for cartilage damage and cell death (Duda et al., 2001; Isaac et al., 2008; Lewis et al., 2003; Milentijevic and Torzilli, 2005; Stolberg-Stolberg et al., 2013; Szczodry et al., 2009). Impact related joint injuries most often occur in car accidents and sports-related impact situations. In sport, accidents to joints typically occur after prior loading of cartilage in a game, while running or skiing etc. However, the effect

of prior loading of cartilage on impact injury and associated cell death has not been studied systematically. Therefore, a realistic experimental set-up mimicking the effects of an impact injury in sport involves a pre-loading protocol prior to impact application.

It is known that static and dynamic loading of cartilage alters the alignment of microstructural components in the tissue and also affects the load distribution between cartilage fluid and matrix phases (Arokoski et al., 1996; Morel et al., 2005; Mukherjee and Wayne, 1998; Park et al., 2003; Soltz and Ateshian, 1998, 2000). These changes may influence the mechanics of cells upon impact loading, and might produce vastly different amounts of cell deaths, depending on the detailed history of cartilage loading prior to impact. Static pre-loading prior to impact has been found to strengthen cartilage and reduce injury (Kim et al., 2012; Morel et al., 2005). On the other hand, the effects of cyclic loading on cartilage damage depend on the amplitude, frequency, and duration (Chen et al., 2003; Ko et al., 2013; Lucchinetti et al., 2002; McCormack and Mansour, 1997; Thibault et al., 2002; Wei et al., 2008; Zimmerman et al., 1988) of the load. While long-term cyclic pre-loading is thought to mechanically stiffen cartilage (Wei et al., 2008), the effects of short-term cyclic pre-loading prior to impact have yet to be explored.

Furthermore, pre-loading of cartilage followed by an injurious or impact load has been performed using externally applied loads through indenters or compression plates. Physiologically-relevant studies, where pre-loading is applied in an intact joint using the natural joint surfaces and muscular loading followed by impact loading, do not exist. But these are the conditions that occur in sport, thus it is important to understand the possible damage to the tissue

114 and to identify pre-load strategies that can be incorporated into warm-up sessions to minimize
115 cartilage damage and chondrocyte death upon possible impact.
116
117 Therefore, the aim of this study was to investigate the effects of joint pre-load history followed
118 by impact loading on chondrocyte death. Experiments were performed in the rabbit
119 patellofemoral joint using two extreme muscular loading conditions: (i) a short-duration maximal
120 intensity muscle loading protocol similar to a 1 repetition, maximal isometric contraction, and (ii)
121 a long-duration low-intensity muscular loading protocol similar to an exhausting running
122 workout. Chondrocyte viability was evaluated following these muscular loading protocols and
123 also following application of a controlled impact load immediately following these muscular pre-
124 loading conditions. Patellofemoral joint contact pressures were also measured for all muscular
125 and impact loading conditions in order to verify if contact pressures could explain potential cell
126 death occurrence. We hypothesized (i) that the short-term and long-term extreme muscular
127 loading conditions produce cell death, (ii) that static and cyclic muscular pre-loads of joints
128 decrease the magnitude of cell death produced by an impact load, and (iii) that the location of
129 cell death occurrence is related to areas of high joint contact pressures during impact loading.
130 With this study, we should be able to answer two important questions: (i) can extreme (high
131 force or long duration) muscular loading cause chondrocyte death in an otherwise healthy and
132 intact joint, and (ii), can certain types of muscular conditioning protocols of the joint alleviate
133 impact-induced chondrocyte death following impact loading.
134
135
136

Methodology

2.1 Animal preparation and loading protocols

All testing was performed on patellofemoral joints from the hind limbs of skeletally mature (1-2 year-old) New Zealand white rabbits (Riemens, St. Agatha, Ontario, Canada) (N_{rabbit} = 42). Rabbits were anaesthetized using a 5% isoflurane-oxygen mixture delivered through mask ventilation, and they were maintained at 2.5% isoflurane throughout the experiment. A bipolar nerve cuff electrode (a silicone tube of 3.4mm in diameter and ~5mm in length, with stainless steel wires on the inside for direct nerve contact) was implanted on the femoral nerve (Longino et al., 2005) of the experimental limb to allow for controlled stimulation of the quadriceps muscles.

After nerve cuff implantation, rabbits were fixed rigidly in a stereotaxic frame using bilateral bone pins in the pelvis and distal femur (Fig. 1a). The knee of the experimental limb was held at 95º of knee flexion. For impact loading, the distal femur was not fixed by bone pins. Instead, the tibia was held vertically by two clamps to allow for centrally-oriented impact loading on the patella using a drop-tower arrangement (Fig. 1b). Once fixed in this position, stimulation of the knee extensor muscles produced isometric knee extensor contractions with associated loading of the patellofemoral joint (Leumann et al., 2013; Ronsky et al., 1995). A strain-gauge-instrumented tibial restraining bar was positioned at the distal end of the tibia to measure the knee extensor forces (Herzog et al., 1998).

Controlled (frequency, duration and magnitude) electrical stimulation to the femoral nerve was delivered through a dual output Grass S8800 stimulator (Astro- MedInc., Longueil, Quebec,

160 Canada). The α-motor neuron threshold of the knee extensor muscles was determined for each
161 rabbit individually by gradually increasing the stimulation voltage of a 200ms pulse train. Once
162 two consecutive increases in stimulation magnitude did not result in a corresponding increase in
163 force, it was established that all motor units of the knee extensor group were activated.
164
165 Once the stimulation threshold and the maximal stimulation magnitude were established, the
166 patellofemoral joints were exposed to different types of muscular loading conditions, as
167 explained in the following:
168 i. Maximal muscle contraction (10s, continuous stimulation)
169 The quadriceps muscles received a 10-second continuous supra-maximal electrical stimulation
170 (4x α-motor neuron threshold, 150Hz, 0.1ms square wave pulse) of the femoral nerve (Herzog
171 and Leonard, 1997) to produce the maximal possible isometric quadriceps loading of the
172 patellofemoral joint.
173 ii. Sub-maximal muscle contraction (3000s, cyclic stimulation)
174 An exhaustive, sub-maximal muscle loading protocol was used to simulate the condition of
175 continuous exercise. The quadriceps muscles were cyclically stimulated to produce 20% of the
176 maximal isometric force for 1500 cycles (500ms on, 1500ms off, 0.1ms square wave pulse). The
177 stimulation current and frequency were adjusted throughout the experiment in order to maintain
178 the muscle force at a constant level. In cases of extreme muscle fatigue (significant drop in
179 muscle force for constant activation conditions), short rest periods (1-2 min) were allowed to
180 regain the muscle force.
181 iii. Impact loading

182 A 1.55kg, 25mm-diameter, flat-ended impactor was dropped from a height of 0.33m onto the
183 center of the patella through a custom-made drop tower in order to deliver a 5J, centrally-
184 oriented, blunt impact load to the patellofemoral joint.
185 iv. Impact loading 1-second after initiation of maximal muscle contraction (pre-1s max,
186 impact)
187 Using a similar set-up as described for conditions (i, iii), a 5J impact load was applied to the
188 patellofemoral joint one second after the initiation of the supra-maximal isometric knee extensor
189 contraction. The electrical stimulation was terminated immediately following the impact loading.
190 v. Impact loading within 5 minutes following submaximal muscle contraction (pre-3000s
191 submax, impact)
192 Using a similar set-up as described for conditions (ii, iii), patellofemoral joints were first sub-
193 maximally loaded by quadriceps muscle contractions for 50-minutes, followed by a 5J impact
194 load (5 minutes).
195
196 Rabbits were sacrificed immediately after the muscular and/or impact loading protocols by a
197 barbiturate overdose using 2ml Euthanyl (pentobarbital sodium, Biomeda-MTC pharmaceuticals,
198 Cambridge, Ontario, Canada). All aspect of animal care and experimental procedures were
199 approved by the University of Calgary's Life Sciences Animal Research and Ethics committee.
200
201 *2.2 Live/dead cell imaging using confocal laser scanning microscopy*
202 Following sacrifice, patellofemoral joints were harvested and fluorescently stained overnight at
203 4°C. Nuclei of live and dead cells were stained with Syto 13 (<10µM, Ex: 488nm; Em: 509nm,
204 Molecular Probe, USA) and SytoX orange (<10µM, Ex: 547nm; Em: 570nm, Molecular Probe,

205 USA), respectively. The patella and femoral groove were then mounted on a petri dish using
206 dental cement. Cell nuclei in the superficial zone cartilage were imaged using a confocal laser
207 scanning microscope (Fluoview FV1000, Olympus, Japan).
208
209 The patella and femoral groove were scanned systematically using a 10x/0.3 NA objective to
210 identify regions of high cell death. These regions and seven pre-defined joint regions in the
211 patellofemoral contact area (Fig. 2) were re-scanned using a 40x/0.8 NA objective to produce
212 images of high resolution for live/dead cell counting. A series of planar images (pixel size:
213 0.62µm x 0.62µm; pixel dwell time: 2.0µs/pixel; field of view: 318µm x 318µm) were acquired
214 along the objective axis (z-axis, i.e., perpendicular to the cartilage surface) at intervals of 0.8µm.
215 Images were taken from the superficial zone and the upper middle zone regions of the cartilage
216 to a depth of 80µm.
217
218 Live/dead cell counting was performed on each image stack (318µm x 318µm x 80µm) using a
219 custom-written Matlab program (Mathworks Inc., Natick, MA). Cell death was expressed as the
220 percentage of dead cells compared to all cells (live and dead) in each image stack. The maximum
221 local cell death was defined by averaging the two image stacks with the highest measured cell
222 death occurrence.
223
224 *2.3 Patellofemoral joint contact pressure measurement*
225 Joint contact pressures were measured using pressure sensitive films (Fuji, Photo Film Ltd.,
226 Tokyo, Japan) of varying grade to account for the wide range of pressures encountered for the
227 different loading conditions. Pressure sensitive film was first calibrated with a series of known

228 forces to produce a standard stain intensity chart (Liggins et al., 1995). An encapsulated strip of
229 pressure film (100mm x 10mm x 0.2mm) (Liggins, 1996) was then inserted into the
230 patellofemoral joint space through bilateral 15mm retinacular incisions (Ronsky et al., 1995).
231 Low-grade pressure film (0-10 MPa) was used for measurement of contact area and low intensity
232 muscular contractions, while medium- (10-50 MPa) and high-grade (>50 MPa) pressure films
233 were used for measurements of peak contact pressures, particularly for the maximal muscular
234 contraction and impact loading conditions. Multiple measurements for each condition were
235 performed with varying grades of pressure sensitive films for accurate measurement of contact
236 areas and peak pressures.
237
238 For simultaneous measurement of cell viability and joint contact pressures during impact loading,
239 impact loading was applied once and contact pressures were measured with the medium-grade
240 pressure sensitive film. The contralateral joints served as unloaded controls and underwent
241 identical procedures, including insertion of the pressure sensitive film, except for the muscular
242 and/or impact loading.
243
244 The stains on the pressure sensitive film produced from joint contact were converted into digital
245 images at a spatial resolution of 0.04 mm. The digital images were modified using ImageJ
246 (National Institute of Health, USA) to account for the granular nature of the Fuji film (Liggins,
247 1996). The magnitude of joint contact pressure was measured by comparing the resulting stain
248 intensity with the standard stain intensity chart. Peak joint contact pressure was defined as the
249 highest average pressure measured over a region of 0.25 mm^2. Joint contact areas were

250 determined from the boundaries of the pressure stains using thresholding methods (Bachus et al.,
251 2006).
252
253 *2.4 Outcome measures and animal grouping*
254 The primary outcome measures in this study were (i) cell viability, and (ii) joint contact
255 areas/pressures. Experiments on cell viability and joint contact pressure were carried out using
256 different animals.
257
258 For the cell viability measurements, 50 patellofemoral joints (N_{joint}) from 26 rabbits were
259 randomly assigned to six loading groups, as follows:
260 a) No loading ($N_{joint} = 13$)
261 b) 10-second continuous maximal muscle loading ($N_{joint} = 14$)
262 c) 3000-second cyclic submaximal muscle loading ($N_{joint} = 6$)
263 d) Impact loading ($N_{joint} = 6$)
264 e) Impact loading 1-second after initiation of maximal muscle loading ($N_{joint} = 5$)
265 f) Impact loading within 5 minutes following 3000-second of cyclic submaximal muscle
266 loading ($N_{joint} = 6$)
267
268 For patellofemoral joint contact pressure measurements, 20 joints (N_{joint}) from ten rabbits were
269 randomly divided into four loading groups, as follows:
270 a) 10-second continuous maximal muscle loading ($N_{joint} = 6$)
271 b) Impact loading ($N_{joint} = 9^{*}$)
272 c) Impact loading 1-second after initiation of maximal muscle loading ($N_{joint} = 9^{*}$)

d) Impact loading within 5 minutes following 3000-second of cyclic submaximal muscle loading ($N_{joint} = 5$)

Groups marked by '*' are from the same joint.

Another set of experiments was performed to measure cell death resulting from blunt impact loading and the corresponding joint contact pressures in the same joint. Six rabbits were used, with the experimental limb receiving the blunt impact loading, while the contralateral limbs served as an unloaded, non-impacted control joints.

2.5 Statistical analysis

All data are presented as means ± 1 standard error of the mean (SEM). Percentage cell death values were compared using parametric two-way ANOVA (with Bonferroni adjustment), while joint contact pressures were compared using non-parametric Kruskal-Wallis testing (with Bonferroni adjustment using Mann-Whitney U test) (α=0.05). (SPSS 20, SPSS Inc., IL, USA).

296 **Results**

297 The maximally-stimulated rabbit quadriceps muscles produced forces of 361±13N; the sub-
298 maximally-stimulated muscles generated average forces of 72±5N. For both extreme muscular
299 loading protocols applied here (the short-duration maximal muscular loading, and the long-
300 duration submaximal muscular loading), we observed a tendency for increased cell death in the
301 cartilage of the patella and femoral groove compared to the corresponding control cartilages of
302 the no-load group animals (Fig. 3). However, only the increase for the high intensity, short
303 duration protocol in the femoral groove reached statistical significance (Fig. 3).

304

305 Blunt impact loading on the rabbit patellofemoral joint caused an increase in the percentage of
306 dead cells compared to the corresponding unloaded control and muscularly-loaded cartilages
307 (Fig. 3-5). Cartilage pre-loaded by a maximal muscular contraction prior to and during impact
308 loading had a decreased percentage of cell death (Fig. 5) compared to the corresponding
309 cartilages receiving impact loading alone (i.e. without any muscular pre-loading). However,
310 cartilage surfaces that were pre-loaded by the 50 minutes of submaximal muscular contractions
311 prior to impact loading showed a vastly increased percentage in cell death compared to animals
312 that received an impact load without any muscular pre-loading of the joint. The percentage of
313 cell death was similar between the patellar and femoral groove cartilages, although femoral
314 groove cartilage experienced a slightly higher percentage of cell death compared to patellar
315 cartilage. In addition to cell death, we also observed tissue cracks caused by the loading
316 protocols, which was reflected in regions of tissue deprived of any cells (Fig. 6).

317

318 Inserting pressure sensitive film into the patellofemoral joints resulted in an increase in the
319 percentage of cell death (8.5±3.0% and 9.0±2.5% in patella and femoral groove, respectively)
320 compared to unloaded control joints (Fig. 3) that were not opened for insertion of pressure
321 sensitive film. Pressure distribution measurements during impact loading revealed that areas of
322 local cell death were not necessarily associated with areas of high contact pressures (Fig. 7).
323
324 Peak pressures in impact-loaded joints (with or without muscular pre-loading) were found to be
325 greater than the corresponding peak pressures of joints loaded by maximal muscular contractions
326 (Fig. 8a). Also, joints that were pre-loaded by maximal muscular contractions prior to impact
327 loading had greater contact areas than joints that were subjected to maximal muscular loading, or
328 to impact loading alone (Fig. 8b). Joints pre-loaded by sub-maximal muscle contractions prior to
329 impact loading had similar contact areas as all the other loading conditions (Fig. 8).
330
331
332
333
334
335
336
337
338
339
340

341 **Discussion:**

342 The effect of impact loading on cell viability has been studied extensively for in situ (Bush et al.,
343 2005; Jeffrey et al., 1995; Krueger et al., 2003; Lewis et al., 2003; Milentijevic and Torzilli,
344 2005; Thambyah et al., 2012) and in vivo (Ewers et al., 2002a; Ewers et al., 2002b; Isaac et al.,
345 2008; Rundell et al., 2005) conditions. The primary focus of the current study was to unravel, for
346 the first time, the effect of in vivo pre-loading on chondrocyte susceptibility to impact injury. In
347 order to achieve this purpose, two extreme pre-loading conditions were used: one representing
348 static maximal intensity muscle contractions, the other representing dynamic long-term (1500
349 cycles) contractions (i.e. about 7 days of rabbit hopping compressed into 50 minutes of exercise)
350 (Horisberger et al., 2012).

351

352 Static maximal intensity muscular loading caused an increase in cell death in femoral groove
353 cartilage (Fig. 3). This result is not necessarily surprising considering that the maximal muscular
354 contractions elicited by nerve stimulation are likely far greater than what a rabbit would be able
355 to generate voluntarily (Basmajian and De Luca, 1985). However, cells in the patella were not
356 affected by such loading, and this result may be attributed to the more compliant nature of
357 patellar compared to femoral groove cartilage (Froimson et al., 1997). Interestingly, high local
358 cell death was observed in the unloaded control group samples from the retropatellar surface.
359 This high cell death may be associated with the spontaneous tissue degradation that has been
360 documented primarily in the distal and middle regions of the rabbit patella (Rehan Youssef et al.,
361 2009), which is also where cell death seemed to be concentrated (mid region of patella) in our
362 study (Fig. 4). Repetitive dynamic sub-maximal muscular loading was also associated with a
363 trend, but not a statistically significant increase, in the percentage of cell death (Fig. 3). Similar

364 results of cell death have been reported before for eccentrically- and concentrically-loaded
365 patellofemoral joints (Horisberger et al., 2012).
366
367 When applying the static pre-conditioning protocol prior to impact loading, we found a small
368 protective effect of the pre-loading (Fig. 5). Although we did not measure tissue strain directly,
369 previous studies (Kim et al., 2012) applying a creep load of 4 MPa for 12 seconds resulted in
370 nominal tissue strains of 16%. Likely, the short (1s) but large (~20 MPa, Fig. 8) static muscular
371 pre-loading in our study has the effect of re-aligning the collagen fibers in cartilage (Kim et al.,
372 2012; Morel et al., 2005), especially in the superficial zone, to follow the shape of the contacting
373 patellofemoral surfaces. As a result, the collagen fibers may be more effective in absorbing the
374 impact load following the pre-load application, thereby alleviating the extent of cell death.
375
376 Surprisingly, the number of dead cells increased dramatically when the pre-loading consisted of
377 the dynamic submaximal muscular loading (Fig. 5). The role played by the interstitial fluid in
378 transmitting load across the cartilage (Mukherjee and Wayne, 1998; Park et al., 2003; Soltz and
379 Ateshian, 1998, 2000) may be a factor in explaining this increase in cell death. The repetitive
380 loading-unloading cycles for 50 minutes likely expelled most of the interstitial fluid from the
381 loaded areas of the superficial zone tissue (Wong et al., 1999). Therefore, chondrocytes in the
382 superficial zone tissue are deprived of the protection afforded by the fluid and the associated
383 hydrostatic pressure. In addition, the loss of interstitial fluid may intensify stress concentrations
384 formed in an incongruent joint (Adams et al., 1999). As a result, the likelihood of cells being
385 injured by impact following long-duration (3000s) dynamic loading of a joint may increase. In
386 contrast, cartilage pre-loaded by a static short-duration (1s) muscular load would be associated

387 with virtually no fluid loss and pressurization of the cartilage prior to impact, thus protection
388 afforded by the fluid phase of the cartilage would be fully available following short-term pre-
389 load conditions.
390
391 Another possible mechanism for the increased cell death occurrence following the sub-maximal
392 dynamic pre-loading could be that cartilage becomes fatigued over the 50-min repetitive
393 muscular preloading protocol. This is insofar a possibility as the loading intensity is extremely
394 high with approximately 1 week of hopping crammed into a 50 minutes loading session.
395 Previous studies found that not only does long-duration cyclic loading lead to a reorientation of
396 the collagen fibers (Arokoski et al., 1996), fatigue induced by cyclic loading of cartilage can also
397 have immediate effects on denaturing collagen fibers and weakening of inter-fibrillar
398 connections (McCormack and Mansour, 1997; Säämämen et al., 1994; Thibault et al., 2002). As
399 a result of such weakening of the collagen fiber network, the tensile strength of cartilage is
400 decreased (McCormack and Mansour, 1997; Thibault et al., 2002). With a reduced protection
401 from the collagen fibers, it is likely that an increased number of cells are exposed to the
402 detrimental effects of impact loading, thus resulting in an increased rate of cell death.
403
404 We also investigated the possible relationship between cell death and joint contact pressures. The
405 peak pressures in impacted joints were generally higher than those found in joints that were
406 loaded by maximal muscle contractions, and impact loading was generally associated with
407 greater cell death percentages than muscular loading (Fig. 3, 5, 8a). However, high contact
408 pressures did not necessarily result in high percentages of cell death (Fig. 7). Cell death appeared
409 to be primarily concentrated at the periphery of the contact area (Fig. 7). These are areas that are

410 typically associated with high shear stresses (Canal et al., 2008; Guterl et al., 2009), therefore
411 this finding suggests that high shear stresses maybe more relevant than peak pressure in causing
412 the observed patterns of cell death. However, we were unable to measure shear stresses with our
413 pressure sensitive film, thus this argument remains speculative and is based on theoretical
414 considerations rather than experimental observations.
415
416 Impact loading causes instantaneous cell necrosis and triggers cell apoptosis through intercellular
417 signaling (Chen et al., 2001b; Levin et al., 2001). The cell deaths observed in our experiments
418 likely contain necrotic and apoptotic cells due to the overnight incubation in the staining solution,
419 and thus the time for apoptosis to take place. As patellar cartilage is softer, but has a higher
420 permeability than femoral groove cartilage (Froimson et al., 1997), it would be expected that the
421 patellar cartilage may exhibit more cell death than the femoral grove cartilage due to the larger
422 cartilage deformation. Instead, we found that there was a slightly (but not statistically significant)
423 increased percentage of dead cells in the femoral groove compared to the patellar cartilage (Fig.
424 3, Fig 5). This finding suggests that the functional properties of cartilage may not be the
425 determining factor for cell death/survival. Differences in morphology of the cell membranes may
426 play a role, as cell membrane unfolding is thought to be associated with impact-induced cell
427 death (Moo et al., 2013; Moo et al., 2012). Also, it is unclear whether cells in this study died
428 mainly of necrosis or apoptosis. Further experiments should be directed towards answering these
429 questions before firm conclusions can be made.
430
431 This study has limitations that need to be considered when interpreting our results. First, only the
432 viability of superficial zone cells was studied due to the limited scanning depth of the confocal

433 microscopy system. Although it is possible to slice the tissue depth-wise in order to measure full-
434 thickness cell viability (Bush et al., 2005; Lewis et al., 2003; Rundell et al., 2005; Stolberg-
435 Stolberg et al., 2013), such an approach was not used here to avoid the artefacts associated with
436 the extraction of cartilage explants and corresponding cell death. However, it has been suggested
437 that cell death caused by impact and other injurious loading is concentrated in the superficial
438 zone tissue (Bush et al., 2005; Duda et al., 2001; Isaac et al., 2008; Rundell et al., 2005). Thus, it
439 is fair to assume that the maximum local cell death was captured in our study. Second, the in
440 vivo muscular loading does not allow for direct measurement of loading rates and tissue strains,
441 although maximal muscular forces in the rabbit quadriceps muscles occur within about 250-
442 300ms, while the peak impact loading was achieved in approximately 2ms. Third, because of the
443 limited range of the pressure sensitive films, loading of joints had to be repeated frequently so as
444 to capture the details of the joint contact pressures. Repeated impact and muscular loading may
445 have altered cartilage properties and thus affected repeat measurements. However, repeat
446 measurements of patellofemoral pressure distributions with identical grade films always gave
447 identical results within the sensitivity and resolution of the Fuji Presensor film (Leumann et al.,
448 2013; Sawatsky et al., 2012). Finally, morphological differences in the tested cartilages and
449 joints, which may have influenced cell viability, were not measured in this study (Lewis et al.,
450 2003). Although the impact load was applied to the centre of the patellofemoral joints in a well-
451 controlled manner and direction, and with a magnitude that did not break underlying bony
452 structures in an attempt to prevent cartilage surface lesions (Ewers et al., 2002b), tissue cracks
453 were observed during the confocal scanning for areas of dead cells (Fig. 6). However, it appears
454 that cell death occurred independent of these tissue cracks in the current study (Fig. 6), which
455 contrasts the findings in the literature where cell death was found to be concentrated near tissue

456 fissures (Ewers et al., 2001; Krueger et al., 2003; Lewis et al., 2003). This difference between
457 our results in the intact knee and those obtained in explant tissue samples is likely due to the
458 differences in the in vivo boundary and loading conditions used here and the ex vivo conditions
459 of previous studies. In the current study, the joint architecture was kept intact, thus preserving the
460 soft tissue contact (cartilage on cartilage) and the natural cartilage on bone structure and function
461 during loading. In contrast, in previous explant studies, the cartilage is artificially removed from
462 its natural environment, its boundaries are changed, and loading occurs through a flat metal
463 indenter, conditions that would be expected to cause the differences in cell viability observed
464 here compared to that published earlier.
465
466 Despite these limitations, the current study provides novel insight into the effects of in vivo pre-
467 loading on cell death in response to impact loading. Future studies should focus on quantifying
468 the morphology of tissue cracks resulting from impact, and the potential relationship between
469 cell death and tissue cracks. The static, 1s maximal muscular pre-loading was associated with
470 protective effects in this study, therefore, future studies should be aimed at finding the optimum
471 magnitude and duration of static muscular loading that can elicit the largest protective effects for
472 cells. However, working with life animals and muscular loading, a 10s static load with supra-
473 maximal nerve stimulation is likely the most static loading that can be applied physiologically, as
474 the quadriceps muscles start to fatigue and lose force rapidly. Finally, the orientation of the
475 collagen fiber network should be measured (Andrews et al., 2014; Chen et al., 2012) pre- and
476 post-loading, to compare differences in load-induced changes in collagen fiber orientation under
477 different loading conditions.
478

In summary, the results of this study led us to the conclusions (i) that joint contact pressures are not tightly associated with cell death occurrence, (ii) that static pre-loading protects cells from impact injury, and (iii) that cyclic/repetitive pre-loading to the point of fatigue leaves the residing chondrocytes vulnerable to injury.

Acknowledgements

The authors declare no financial or personal relationship with other people or organizations that could inappropriately influence or bias this work. The authors would like to express gratitude to Dr. Tak-Shing Fung for his help in statistical analysis. This work was supported by grants from the Canadian Institutes of Health Research, The Canada Research Chair Programme, and the Killam Foundation.

References

Adams, M.A., Kerinv, A.J., Bhatia, L.S., Chakrabarty, G., Dolan, P., 1999. Experimental determination of stress distributions in articular cartilage before and after sustained loading. Clinical Biomechanics 14, 88-96.

Aigner, T., Söder, S., Gebhard, P.M., McAlinden, A., Haag, J., 2007. Mechanisms of Disease: role of chondrocytes in the pathogenesis of osteoarthritis—structure, chaos and senescence. Nature Reviews Rheumatology 3, 391-399.

Anderson, D.D., Chubinskaya, S., Guilak, F., Martin, J.A., Oegema, T.R., Olson, S.A., Buckwalter, J.A., 2011. Post-traumatic osteoarthritis: Improved understanding and opportunities for early intervention. Journal of Orthopaedic Research 29, 802-809.

Andrews, S.H.J., Rattner, J.B., Abusara, Z., Adesida, A., Shrive, N.G., Ronsky, J.L., 2014. Tie-fibre structure and organization in the knee menisci. Journal of Anatomy 224, 531-537.

Arokoski, J.P., Hyttinen, M.M., Lapveteläinen, T., Takács, P., Kosztáczky, B., Módis, L., Kovanen, V., Helminen, H., 1996. Decreased birefringence of the superficial zone collagen network in the canine knee (stifle) articular cartilage after long distance running training, detected by quantitative polarised light microscopy. Annals of the Rheumatic Diseases 55, 253-264.

Bachus, K.N., DeMarco, A.L., Judd, K.T., Horwitz, D.S., Brodke, D.S., 2006. Measuring contact area, force, and pressure for bioengineering applications: Using Fuji Film and TekScan systems. Medical Engineering & Physics 28, 483-488.

Basmajian, J.V., De Luca, C.J., 1985. Muscles Alive: Their Functions Revealed by Electromyography, 5th ed. Williams & Wilkins, Baltimore.

Blanco, F.J., Guitian, R., Vázquez-Martul, E., de Toro, F.J., Galdo, F., 1998. Osteoarthritis chondrocytes die by apoptosis. A possible pathway for osteoarthritis pathology. Arthritis and Rheumatism 41, 284-289.

Bush, P.G., Hodkinson, P.D., Hamilton, G.L., Hall, A.C., 2005. Viability and volume of in situ bovine articular chondrocytes-changes following a single impact and effects of medium osmolarity. Osteoarthritis and Cartilage 13, 54-65.

Canal, C.E., Hung, C.T., Ateshian, G.A., 2008. Two-Dimensional Strain Fields on the Cross-Section of the Bovine Humeral Head Under Contact Loading. Journal of Biomechanics 41, 3145-3151.

Chen, C.-T., Bhargava, M., Lin, P.M., Torzilli, P.A., 2003. Time, stress, and location dependent chondrocyte death and collagen damage in cyclically loaded articular cartilage. Journal of Orthopaedic Research 21, 888-898.

Chen, C.T., Burton-Wurster, N., Borden, C., Hueffer, K., Bloom, S.E., Lust, G., 2001a. Chondrocyte necrosis and apoptosis in impact damaged articular cartilage. Journal of Orthopaedic Research 19, 703-711.

Chen, C.T., Burton-Wurster, N., Borden, C., Hueffer, K., Bloom, S.E., Lust, G., 2001b. Chondrocyte necrosis and apoptosis in impact damaged articular cartilage. Journal of Orthopaedic Research: Official Publication of the Orthopaedic Research Society 19, 703-711.

Chen, X., Nadiarynkh, O., Plotnikov, S., Campagnola, P.J., 2012. Second harmonic generation microscopy for quantitative analysis of collagen fibrillar structure. Nat. Protocols 7, 654-669.

Dirschl, D.R., Marsh, L.J., Buckwalter, J.A., Gelberman, R., Olson, S.A., Brown, T.D., Llinias, A., 2004. Articular Fractures. Journal of the American Academy of Orthopaedic Surgeons November 12, 416-423.

547 Duda, G.N., Eilers, M., Loh, L., Hoffman, J.E., Kääb, M., Schaser, K., 2001. Chondrocyte death
548 precedes structural damage in blunt impact trauma. Clinical Orthopaedics and Related
549 Research, 302-309.
550 Ewers, B.J., Dvoracek-Driksna, D., Orth, M.W., Haut, R.C., 2001. The extent of matrix damage
551 and chondrocyte death in mechanically traumatized articular cartilage explants depends on
552 rate of loading. Journal of Orthopaedic Research 19, 779-784.
553 Ewers, B.J., Jayaraman, V.M., Banglmaier, R.F., Haut, R.C., 2002a. Rate of blunt impact loading
554 affects changes in retropatellar cartilage and underlying bone in the rabbit patella. Journal of
555 Biomechanics 35, 747-755.
556 Ewers, B.J., Weaver, B.T., Haut, R.C., 2002b. Impact orientation can significantly affect the
557 outcome of a blunt impact to the rabbit patellofemoral joint. Journal of Biomechanics 35,
558 1591-1598.
559 Froimson, M.I., Ratcliffe, A., Gardner, T.R., Mow, V.C., 1997. Differences in patellofemoral
560 joint cartilage material properties and their significance to the etiology of cartilage surface
561 fibrillation. Osteoarthritis and Cartilage 5, 377-386.
562 Guterl, C.C., Gardner, T.R., Rajan, V., Ahmad, C.S., Hung, C.T., Ateshian, G.A., 2009. Two-
563 dimensional strain fields on the cross-section of the human patellofemoral joint under
564 physiological loading. Journal of Biomechanics 42, 1275-1281.
565 Hashimoto, S., Ochs, R.L., Komiya, S., Lotz, M., 1998. Linkage of chondrocyte apoptosis and
566 cartilage degradation in human osteoarthritis. Arthritis and Rheumatism 41, 1632-1638.
567 Herzog, W., Diet, S., Suter, E., Mayzus, P., Leonard, T.R., Müller, C., Wu, J.Z., Epstein, M.,
568 1998. Material and functional properties of articular cartilage and patellofemoral contact
569 mechanics in an experimental model of osteoarthritis. Journal of Biomechanics 31, 1137-1145.
570 Herzog, W., Leonard, T.R., 1997. Depression of cat soleus forces following isokinetic shortening.
571 Journal of Biomechanics 30, 865-872.
572 Horisberger, M., Fortuna, R., Leonard, T.R., Valderrabano, V., Herzog, W., 2012. The influence
573 of cyclic concentric and eccentric submaximal muscle loading on cell viability in the rabbit
574 knee joint. Clinical Biomechanics (Bristol, Avon) 27, 292-298.
575 Isaac, D.I., Meyer, E.G., Haut, R.C., 2008. Chondrocyte damage and contact pressures following
576 impact on the rabbit tibiofemoral joint. Journal of Biomechanical Engineering 130, 041018-
577 041011-041015.
578 Jeffrey, J.E., Gregory, D.W., Aspden, R.M., 1995. Matrix damage and chondrocyte viability
579 following a single impact load on articular cartilage. Archives of Biochemistry and
580 Biophysics 322, 87-96.
581 Kim, W., Thambyah, A., Broom, N., 2012. Does prior sustained compression make cartilage-on-
582 bone more vulnerable to trauma? Clinical Biomechanics (Bristol, Avon) 27, 637-645.
583 Ko, F.C., Dragomir, C., Plumb, D.A., Goldring, S.R., Wright, T.M., Goldring, M.B., van der
584 Meulen, M.C.H., 2013. In vivo cyclic compression causes cartilage degeneration and
585 subchondral bone changes in mouse tibiae. Arthritis & Rheumatism 65, 1569-1578.
586 Krueger, J.A., Thisse, P., Ewers, B.J., Dvoracek-Driksna, D., Orth, M.W., Haut, R.C., 2003. The
587 extent and distribution of cell death and matrix damage in impacted chondral explants varies
588 with the presence of underlying bone. Journal of Biomechanical Engineering 125, 114-119.
589 Leumann, A., Fortuna, R., Leonard, T., Valderrabano, V., Herzog, W., 2013. Dynamic in-vivo
590 force transfer in the lapine knee loaded by quadriceps muscle contraction. Clinical
591 Biomechanics 28, 199-204.

592 Levin, A., Burton-Wurster, N., Chen, C.T., Lust, G., 2001. Intercellular signaling as a cause of
593 cell death in cyclically impacted cartilage explants. Osteoarthritis and Cartilage 9, 702-711.
594 Lewis, J.L., Deloria, L.B., Oyen-Tiesma, M., Thompson, R.C.J., Ericson, M., Oegema, T.R.J.,
595 2003. Cell death after cartilage impact occurs around matrix cracks. Journal of Orthopaedic
596 Research 21, 881-887.
597 Liggins, A.B., 1996. The practical application of Fuji Prescale pressure-sensitive film, in: Orr,
598 J.F., Shelton, J.C. (Eds.), Optical measurement methods in biomechanics. Springer US, pp.
599 173-189.
600 Liggins, A.B., Hardie, W.R., Finlay, J.B., 1995. The spatial and pressure resolution of fuji
601 pressure-sensitive film. Experimental Mechanics 35, 166-173.
602 Longino, D., Butterfield, T.A., Herzog, W., 2005. Frequency and length-dependent effects of
603 Botulinum toxin-induced muscle weakness. Journal of Biomechanics 38, 609-613.
604 Lucchinetti, E., Adams, C.S., Horton Jr, W.E., Torzilli, P.A., 2002. Cartilage viability after
605 repetitive loading: a preliminary report. Osteoarthritis and Cartilage 10, 71-81.
606 McCormack, T., Mansour, J.M., 1997. Reduction in tensile strength of cartilage precedes surface
607 damage under repeated compressive loading in vitro. Journal of Biomechanics 31, 55-61.
608 Milentijevic, D., Torzilli, P.A., 2005. Influence of stress rate on water loss, matrix deformation
609 and chondrocyte viability in impacted articular cartilage. Journal of Biomechanics 38, 493-
610 502.
611 Moo, E.K., Amrein, M., Epstein, M., Duvall, M., Abu Osman, N.A., Pingguan-Murphy, B.,
612 Herzog, W., 2013. The Properties of Chondrocyte Membrane Reservoirs and Their Role in
613 Impact-Induced Cell Death. Biophysical Journal 105, 1590-1600.
614 Moo, E.K., Herzog, W., Han, S.K., Abu Osman, N.A., Pingguan-Murphy, B., Federico, S., 2012.
615 Mechanical behaviour of in-situ chondrocytes subjected to different loading rates: a finite
616 element study. Biomechanics and Modeling in Mechanobiology 11, 983-993.
617 Morel, V., Merçay, A., Quinn, T.M., 2005. Prestrain decreases cartilage susceptibility to injury
618 by ramp compression in vitro. Osteoarthritis and Cartilage 13, 964-970.
619 Mukherjee, N., Wayne, J.S., 1998. Load Sharing Between Solid and Fluid Phases in Articular
620 Cartilage: II — Comparison of Experimental Results and u-p Finite Element Predictions.
621 Journal of Biomechanical Engineering 120, 620-624.
622 Park, S., Krishnan, R., Nicoll, S.B., Ateshian, G.A., 2003. Cartilage Interstitial Fluid Load
623 Support in Unconfined Compression. Journal of Biomechanics 36, 1785-1796.
624 Rehan Youssef, A., Longino, D., Seerattan, R., Leonard, T., Herzog, W., 2009. Muscle weakness
625 causes joint degeneration in rabbits. Osteoarthritis and Cartilage 17, 1228-1235.
626 Ronsky, J.L., Herzog, W., Brown, T.D., Pedersen, D.R., Grood, E.S., Butler, D.L., 1995. In vivo
627 quantification of the cat patellofemoral joint contact stresses and areas. Journal of
628 Biomechanics 28, 977-983.
629 Rundell, S.A., Baars, D.C., Phillips, D.M., Haut, R.C., 2005. The limitation of acute necrosis in
630 retro-patellar cartilage after a severe blunt impact to the in vivo rabbit patello-femoral joint.
631 Journal of Orthopaedic Research 23, 1363-1369.
632 Säämämen, A.M., Kiviranta, I., Jurvelin, J., Helminen, H.J., Tammi, M., 1994. Proteoglycan and
633 collagen alterations in canine knee articular cartilage following 20 km daily running exercise
634 for 15 weeks. Connective Tissue Research 30, 191-201.
635 Sawatsky, A., Bourne, D., Horisberger, M., Jinha, A., Herzog, W., 2012. Changes in
636 patellofemoral joint contact pressures caused by vastus medialis muscle weakness. Clinical
637 Biomechanics 27, 595-601.

638 Shlopov, B.V., Lie, W.R., Mainardi, C.L., Cole, A.A., Chubinskaya, S., Hasty, K.A., 1997.
639 Osteoarthritic Lesions. Involvement of three different collagenases. Arthritis & Rheumatism
640 40, 2065-2074.
641 Soltz, M.A., Ateshian, G.A., 1998. Experimental verification and theoretical prediction of
642 cartilage interstitial fluid pressurization at an impermeable contact interface in confined
643 compression. Journal of Biomechanics 31, 927-934.
644 Soltz, M.A., Ateshian, G.A., 2000. Interstitial fluid pressurization during confined compression
645 cyclical loading of articular cartilage. Annals of Biomedical Engineering 28, 150-159.
646 Stolberg-Stolberg, J.A., Furman, B.D., William Garrigues, N., Lee, J., Pisetsky, D.S., Stearns,
647 N.A., DeFrate, L.E., Guilak, F., Olson, S.A., 2013. Effects of cartilage impact with and
648 without fracture on chondrocyte viability and the release of inflammatory markers. Journal of
649 Orthopaedic Research 31, 1283-1292.
650 Szczodry, M., Coyle, C.H., Kramer, S.J., Smolinski, P., Chu, C.R., 2009. Progressive
651 chondrocyte death after impact injury indicates a need for chondroprotective therapy. The
652 American Journal of Sports Medicine 37, 2318-2322.
653 Thambyah, A., Zhang, G., Kim, W., Broom, N.D., 2012. Impact induced failure of cartilage-on-
654 bone following creep loading: A microstructural and fracture mechanics study. Journal of the
655 Mechanical Behavior of Biomedical Materials 14, 239-247.
656 Thibault, M., Poole, A.R., Buschmann, M.D., 2002. Cyclic compression of cartilage/bone
657 explants in vitro leads to physical weakening, mechanical breakdown of collagen and release
658 of matrix fragments. Journal of Orthopaedic Research 20, 1265-1273.
659 Wei, F., Golenberg, N., Kepich, E.T., Haut, R.C., 2008. Effect of intermittent cyclic preloads on
660 the response of articular cartilage explants to an excessive level of unconfined compression.
661 Journal of Orthopaedic Research 26, 1636-1642.
662 Wieland, H.A., Michaelis, M., Kirschbaum, B.J., Rudolphi, K.A., 2005. Osteoarthritis - an
663 untreatable disease? Nat Rev Drug Discov 4, 331-344.
664 Wong, M., Siegrist, M., Cao, X., 1999. Cyclic compression of articular cartilage explants is
665 associated with progressive consolidation and altered expression pattern of extracellular
666 matrix proteins. Matrix Biology 18, 391-399.
667 Zimmerman, N.B., Smith, D.G., Pottenger, L.A., Cooperman, D.R., 1988. Mechanical disruption
668 of human patellar cartilage by repetitive loading in vitro. Clinical Orthopaedics and Related
669 Research, 302-307.

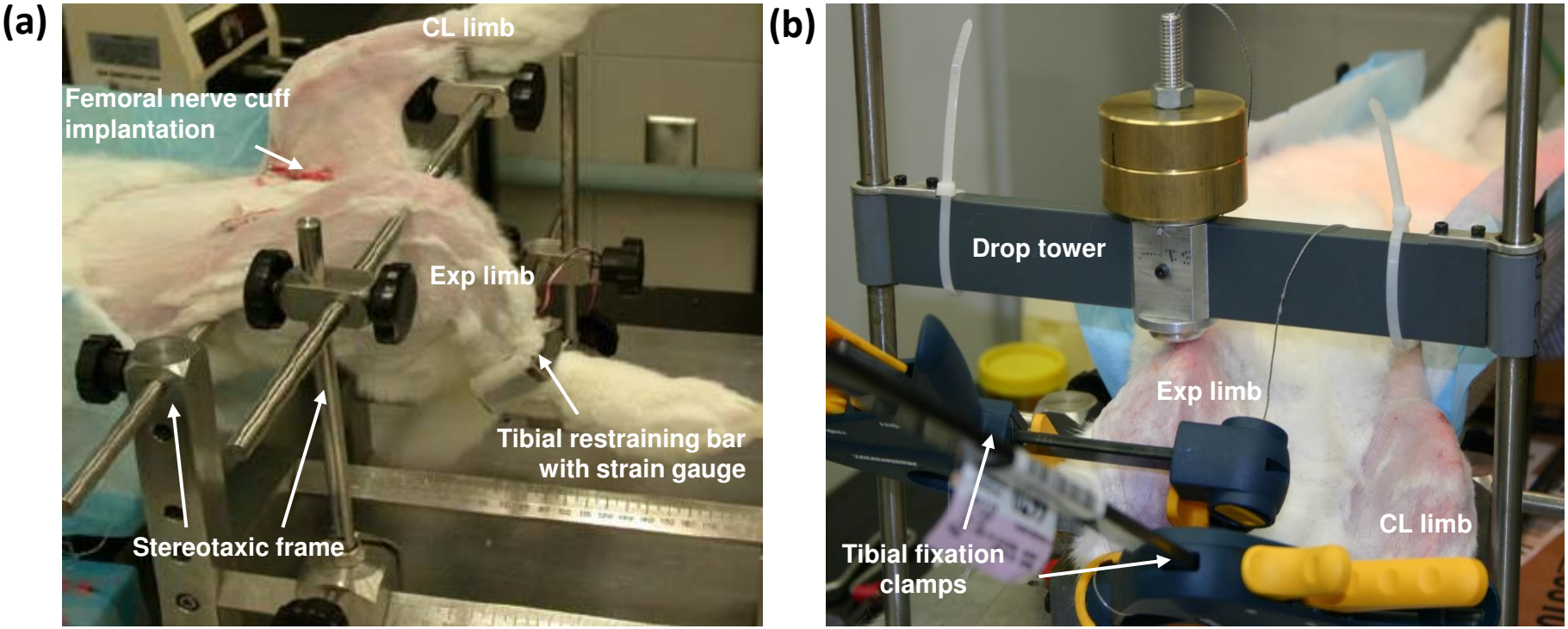

*** Exp limb – experimental limb**

*** CL limb – contralateral limb**

Fig. 1. Experimental set up used for loading of lapine patellofemoral joints. (a) Controlled muscular loading. Rabbits were fixed in a stereotaxic frame using bilateral bone pins at the pelvis and distal femur. The quadriceps muscle group was stimulated through an implanted femoral nerve cuff (Longino et al., 2005). An instrumented tibial restraining bar was used to measure the resulting isometric muscle forces (Herzog et al., 1998). (b) Impact loading was applied using a drop tower. Rabbits were fixed as described in (a), but the distal femur was not fixed. Instead, the tibia was clamped vertically to allow for centrally-oriented impact loading on the patella.

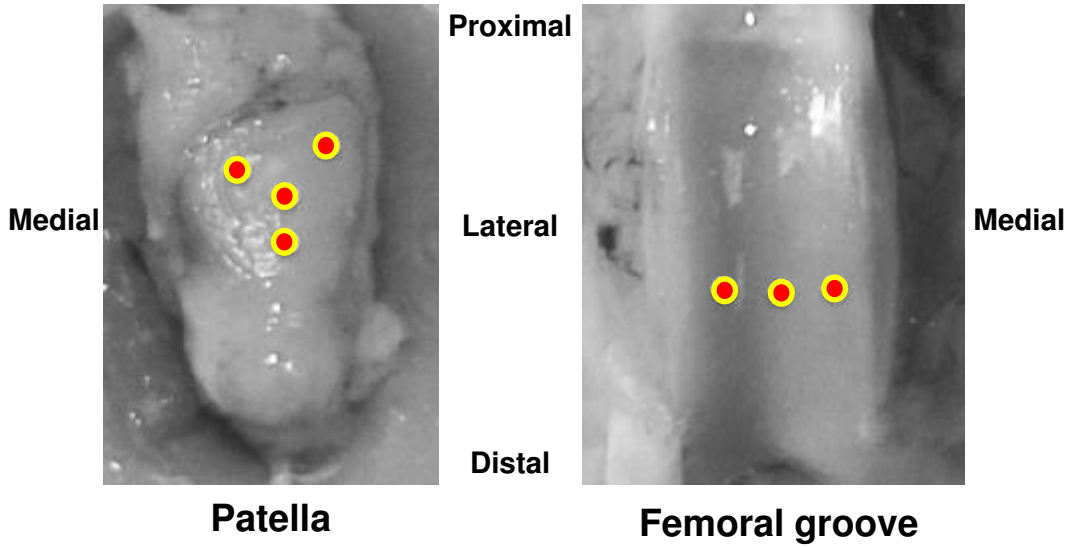

ig. 2. Pre-defined scanning regions corresponding to areas of patellofemoral contact.

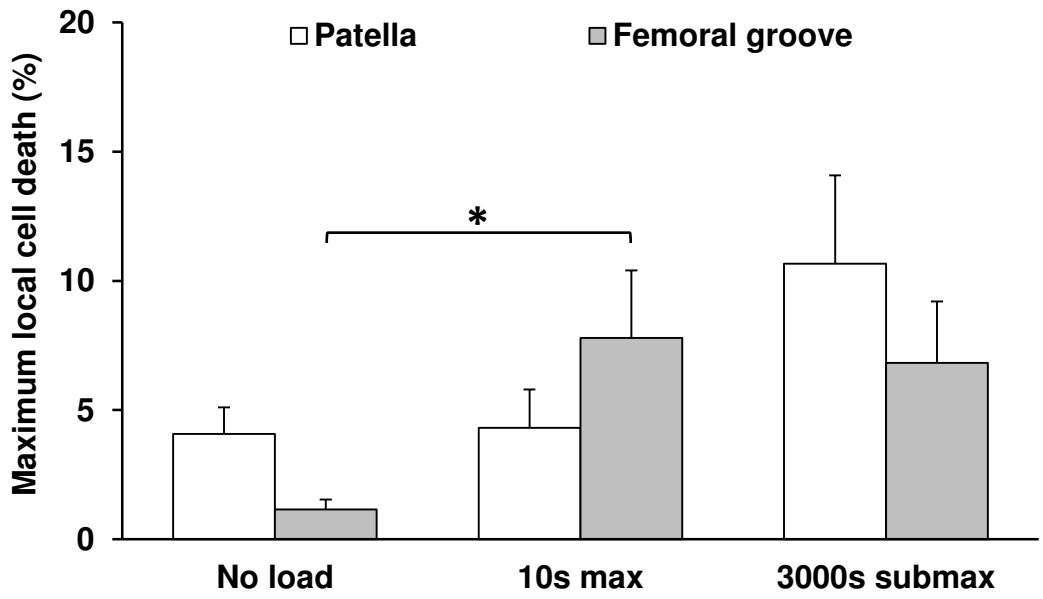

Fig. 3. The effect of extreme muscular loading on cell viability in patella and femoral groove cartilages. A 10-second continuous maximal muscular loading was found to cause increased cell death in femoral groove compared to unloaded control cartilage. Due to the relatively high cell death in patellar cartilage of control group animals, cell death in the patella for the long-duration submaximal muscular loading was not statistically different from control group values. The marking '*' indicates a significant difference in cell death ($p<0.05$).

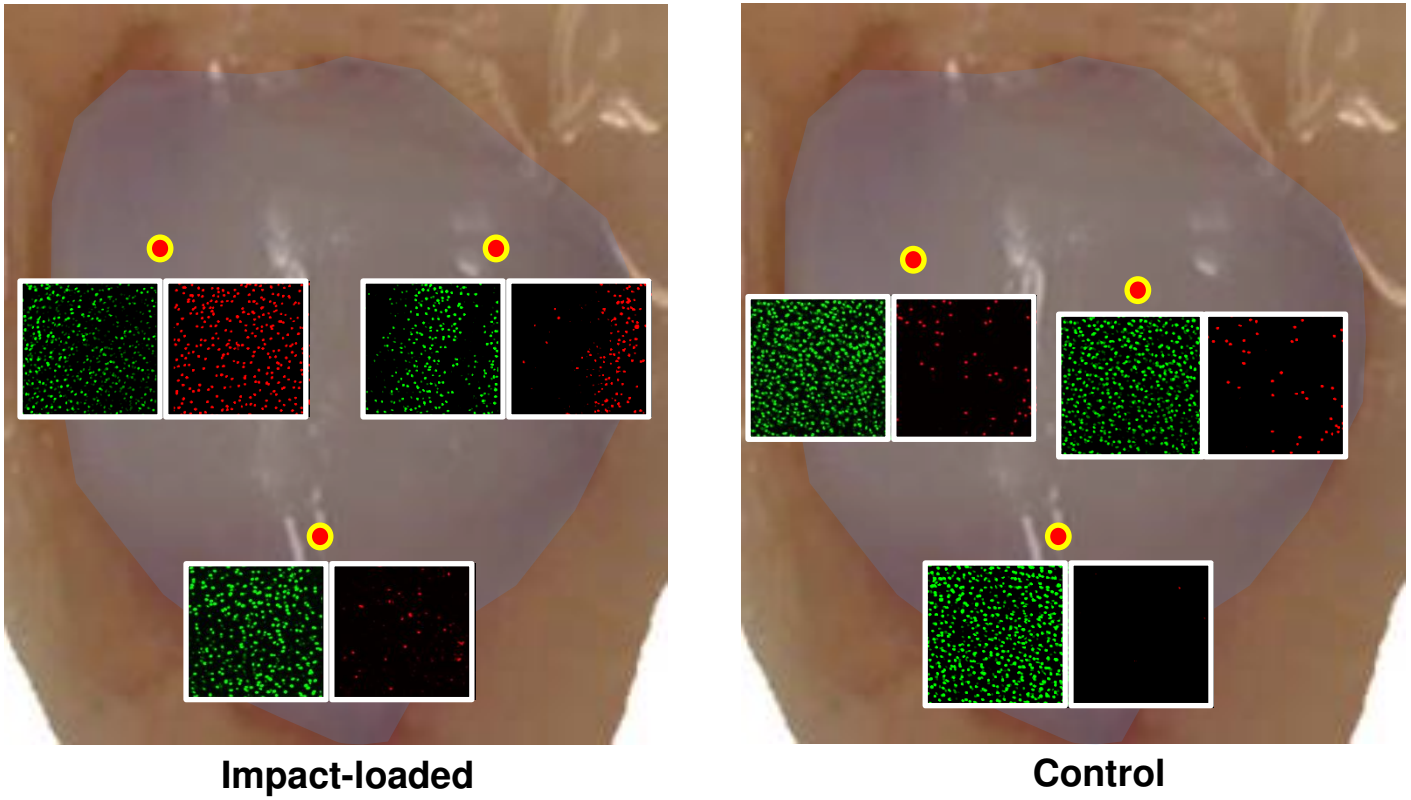

Fig. 4. Example showing cell viability through live/dead cell imaging at different regions of the retropatellar cartilage (highlighted in light blue) receiving impact load (left) and no load (right). In each region, the image stack of live/dead cells was projected onto a single plane, thus resulting in the appearance of a dense cell population. Two windows are presented for each joint location (marked by the red circle), with the left window showing the live cells (green dots), while the right window shows the dead cells (red dots).

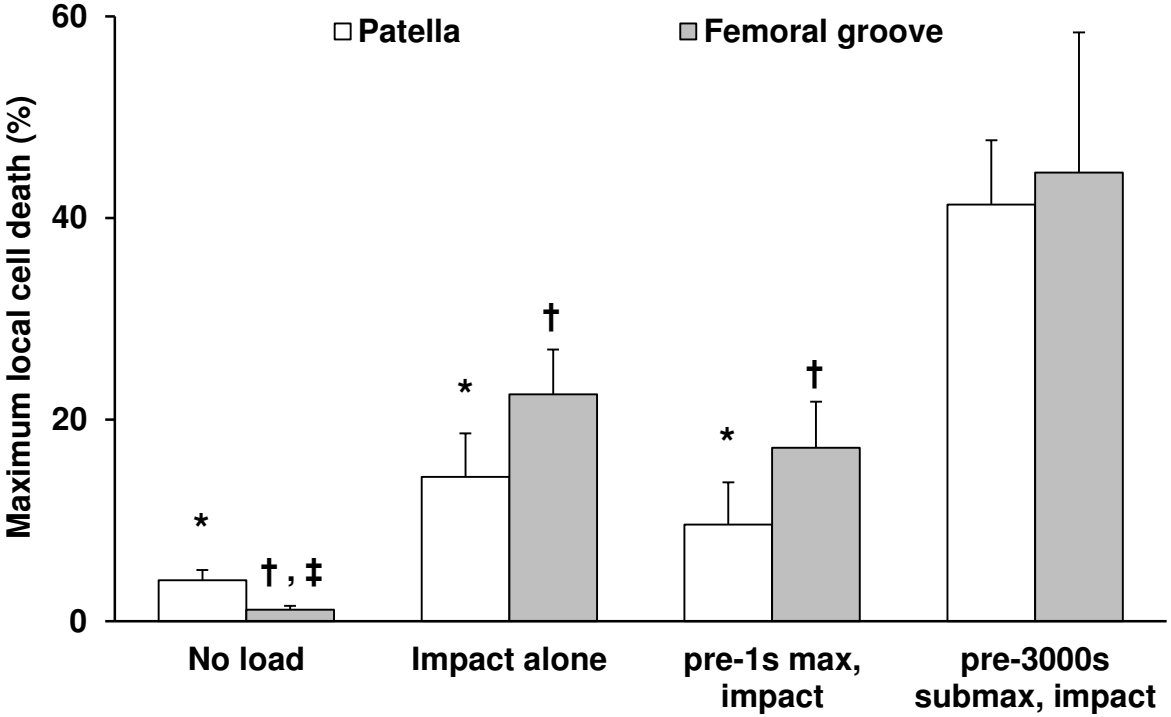

Fig. 5. The effect of muscular pre-loading on impact-induced cell death. Blunt impact loading alone resulted in increased cell death in femoral groove cartilage when compared to the no load control condition. Pre-loading the patellofemoral joint with a maximal muscular contraction for 1s prior to and during the impact loading was associated with a decrease in the percentage of dead cells compared to impact loading alone (not statistically significant), suggesting a protective effect of this type of pre-loading. In contrast, cyclic submaximal muscular contractions for 3000s prior to impact loading increased the percentage of cell death significantly compared to impact loading alone, implying that this type of pre-loading makes chondrocytes more vulnerable to an impact load. The marking '*', '†' indicates a significant difference in the percentage of cartilage cell death compared to patella and femoral groove in the 'pre-3000s submax, impact' group, respectively ($p<0.05$). The marking '‡' indicates a significant difference in the percentage of cartilage cell death compared to the femoral groove in the 'impact alone' group.

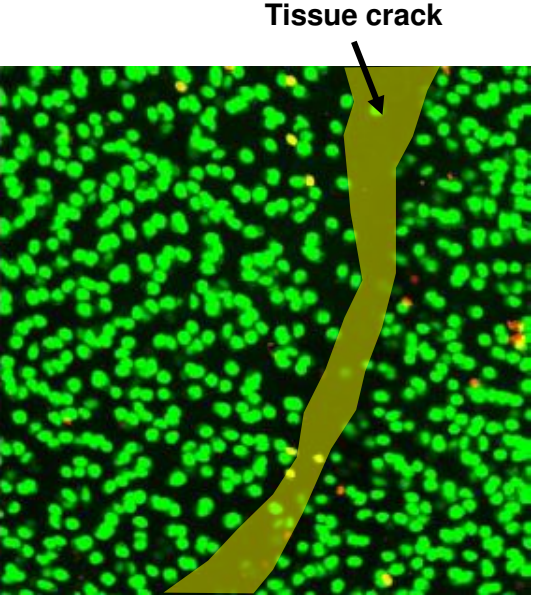

mple of a tissue crack (highlighted in yellow) induced by continuous maximal muscle loading. The tissue crack under confocal microscopy as tissue region deprived of ytes. This image represents a tissue area of 0.10mm^2 rated by projecting all the planar images constituting the me onto a single plane. The green dots represent live red dots indicate dead cells.

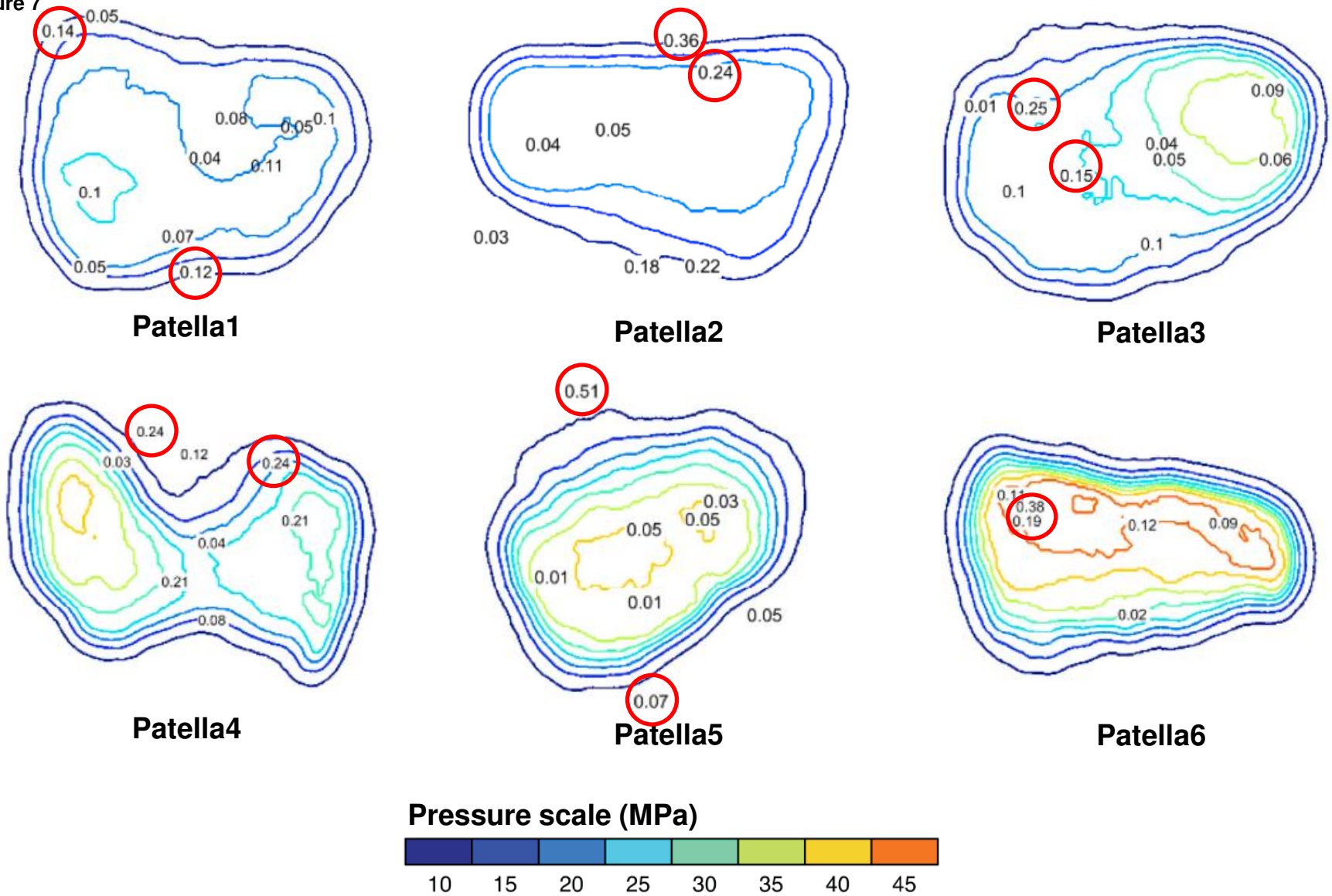

Fig. 7. Contour plots of pressure distribution on patellar cartilage during blunt impact loading. Since the insertion of pressure sensitive film into the patellofemoral joint was associated with an increase in cell death, examination of the relationship between contact pressure and cell viability had to be carried out using a separate set of experiments. Local cell death normalized to total number of cells (indicated by the numeric values) was co-localized with the pressure contour plots to show the relationship between local cell death occurrence and local joint pressures. The two regions of highest cell death were circled in red for each patella. From these results, it appears that cell death is not related to high contact pressures (e.g. patella 2 and patella 5).

Figure 8

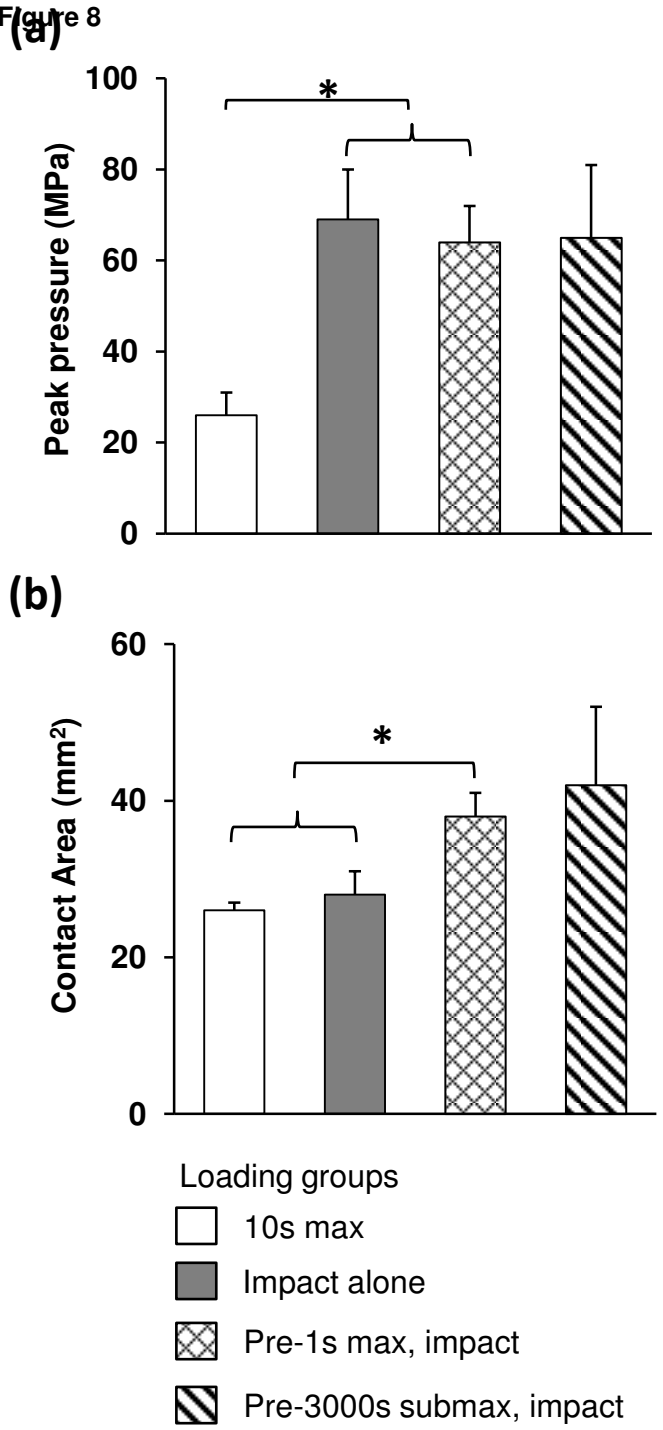

Fig. 8. Peak pressures (a) and contact areas (b) for the patellofe
joint under the experimental loading conditions. Joints pre-loadec
1s maximal muscular contraction have greater contact areas, but
cell death percentages (in Fig. 3), than joints subjected to ir
loading alone. The marking '*' indicates a significant difference i
death ($p<0.05$).

Legends for figures

Fig. 1. Experimental set up used for loading of lapine patellofemoral joints. (a) Controlled muscular loading. Rabbits were fixed in a stereotaxic frame using bilateral bone pins at the pelvis and distal femur. The quadriceps muscle group was stimulated through an implanted femoral nerve cuff (Longino et al., 2005). An instrumented tibial restraining bar was used to measure the resulting isometric muscle forces (Herzog et al., 1998). (b) Impact loading was applied using a drop tower. Rabbits were fixed as described in (a), but the distal femur was not fixed. Instead, the tibia was clamped vertically to allow for centrally-oriented impact loading on the patella.

Fig. 2. Pre-defined scanning regions corresponding to areas of patellofemoral contact.

Fig. 3. The effect of extreme muscular loading on cell viability in patella and femoral groove cartilages. A 10-second continuous maximal muscular loading was found to cause increased cell death in femoral groove compared to unloaded control cartilage. Due to the relatively high cell death in patellar cartilage of control group animals, cell death in the patella for the long-duration submaximal muscular loading was not statistically different from control group values. The marking '*' indicates a significant difference in cell death ($p<0.05$).

Fig. 4. Example showing cell viability through live/dead cell imaging at different regions of the retropatellar cartilage (highlighted in light blue) receiving impact load (left) and no load (right). In each region, the image stack of live/dead cells was projected onto a single plane, thus resulting in the appearance of a dense cell population. Two windows are presented for each joint location

(marked by the red circle), with the left window showing the live cells (green dots), while the right window shows the dead cells (red dots).

Fig. 5. The effect of muscular pre-loading on impact-induced cell death. Blunt impact loading alone resulted in increased cell death in femoral groove cartilage when compared to the no load control condition. Pre-loading the patellofemoral joint with a maximal muscular contraction for 1s prior to and during the impact loading was associated with a decrease in the percentage of dead cells compared to impact loading alone (not statistically significant), suggesting a protective effect of this type of pre-loading. In contrast, cyclic submaximal muscular contractions for 3000s prior to impact loading increased the percentage of cell death significantly compared to impact loading alone, implying that this type of pre-loading makes chondrocytes more vulnerable to an impact load. The marking '*', '†' indicates a significant difference in the percentage of cartilage cell death compared to patella and femoral groove in the 'pre-3000s submax, impact' group, respectively ($p<0.05$). The marking '‡' indicates a significant difference in the percentage of cartilage cell death compared to the femoral groove in the 'impact alone' group.

Fig. 6. An example of a tissue crack (highlighted in yellow) induced by a 10-second continuous maximal muscle loading. The tissue crack was observed under confocal microscopy as tissue region deprived of any chondrocytes. This image represents a tissue area of $0.10mm^2$ and was generated by projecting all the planar images constituting the scanned volume onto a single plane. The green dots represent live cells while the red dots indicate dead cells.

Fig. 7. Contour plots of pressure distribution on patellar cartilage during blunt impact loading. Since the insertion of pressure sensitive film into the patellofemoral joint was associated with an increase in cell death, examination of the relationship between contact pressure and cell viability had to be carried out using a separate set of experiments. Local cell death normalized to total number of cells (indicated by the numeric values) was co-localized with the pressure contour plots to show the relationship between local cell death occurrence and local joint pressures. The two regions of highest cell death were circled in red for each patella. From these results, it appears that cell death is not related to high contact pressures (e.g. patella 2 and patella 5).

Fig. 8. Peak pressures (a) and contact areas (b) for the patellofemoral joint under the experimental loading conditions. Joints pre-loaded with 1s maximal muscular contraction have greater contact areas, but lower cell death percentages (in Fig. 3), than joints subjected to impact loading alone. The marking '*' indicates a significant difference in cell death ($p<0.05$).